

## Phase-Driving Hole Spin Qubits

Stefano Bosco<sup>1,\*</sup>, Simon Geyer<sup>1</sup>, Leon C. Camenzind<sup>1,†</sup>, Rafael S. Eggl<sup>1</sup>, Andreas Fuhrer,<sup>2</sup>

Richard J. Warburton,<sup>1</sup> Dominik M. Zumbühl<sup>1</sup>, J. Carlos Egues<sup>1,3</sup>, Andreas V. Kuhlmann<sup>1</sup>, and Daniel Loss<sup>1</sup>

<sup>1</sup>Department of Physics, University of Basel, Klingelbergstrasse 82, 4056 Basel, Switzerland

<sup>2</sup>IBM Research Europe-Zurich, Säumerstrasse 4, CH-8803 Rüschlikon, Switzerland

<sup>3</sup>Instituto de Física de São Carlos, Universidade de São Paulo, 13560-970 São Carlos, São Paulo, Brazil



(Received 18 March 2023; accepted 3 October 2023; published 7 November 2023)

The spin-orbit interaction in spin qubits enables spin-flip transitions, resulting in Rabi oscillations when an external microwave field is resonant with the qubit frequency. Here, we introduce an alternative driving mechanism mediated by the strong spin-orbit interactions in hole spin qubits, where a far-detuned oscillating field couples to the qubit phase. Phase-driving at radio frequencies, orders of magnitude slower than the microwave qubit frequency, induces highly nontrivial spin dynamics, violating the Rabi resonance condition. By using a qubit integrated in a silicon fin field-effect transistor, we demonstrate a controllable suppression of resonant Rabi oscillations and their revivals at tunable sidebands. These sidebands enable alternative qubit control schemes using global fields and local far-detuned pulses, facilitating the design of dense large-scale qubit architectures with local qubit addressability. Phase-driving also decouples Rabi oscillations from noise, an effect due to a gapped Floquet spectrum and can enable Floquet engineering high-fidelity gates in future quantum processors.

DOI: 10.1103/PhysRevLett.131.197001

**Introduction.**—Spin qubits in hole quantum dots are emerging as top candidates to build large-scale quantum processors [1–4]. A key advantage of hole spins is their large and tunable spin-orbit interaction (SOI) enabling ultrafast all-electrical qubit operations [5–12], on-demand coupling to microwave photons [13–15], even without bulky micro-magnets [16–18]. The large SOI of holes leads to interesting physical phenomena, such as electrically tunable Zeeman [6,19–23] and hyperfine interactions [24–26], or exchange anisotropies at finite [27] and zero magnetic fields [28,29]. These effects can be leveraged for quantum information processing, e.g., to define operational sweet spots against noise [30–35].

Single qubit operations rely on manipulating spin states on demand. A microwave pulse drives spin rotations, resulting in the well-known Rabi oscillations. For confined holes, these oscillations are fast and rely on either an electrically tunable and anisotropic  $g$  tensor [36–38] or periodic spin motion in a SOI field [39–42]. To date, however, these oscillations are qualitatively similar to competing qubit architectures [43–47], and they occur at fixed microwave GHz frequencies determined by the qubit energy. Qubit responses to detuned frequencies are associated to nonlinearities in the coupling to the driving field [48,49].

In this Letter, we investigate the dynamics of a hole spin qubit hosted in a silicon fin field-effect transistor (Si FinFET) under simultaneous application of longitudinal (phase) and transverse (Rabi) drives at radio-frequency  $\omega_z$  and microwave frequency  $\omega_x$ , respectively, see Fig. 1(a).

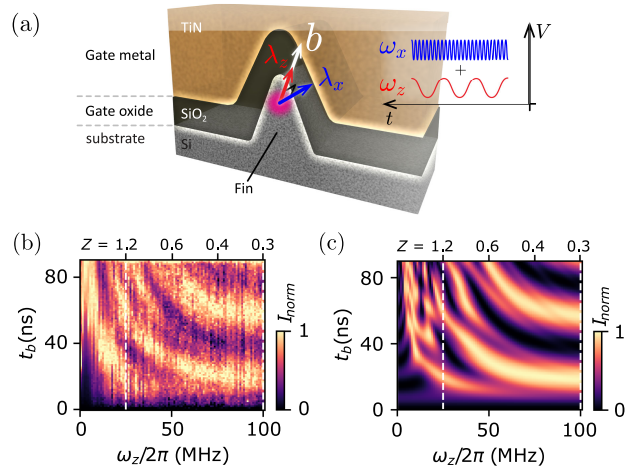


FIG. 1. (a) Schematic of our phase-driven qubit. A hole spin qubit in a Si FinFET with Zeeman field  $\mathbf{b}$  is simultaneously driven by a microwave Rabi drive (blue) with amplitude  $\lambda_x$  and frequency  $\omega_x \approx \omega_q = |\mathbf{b}|/\hbar$  and a radio-frequency phase drive (red) with amplitude  $\lambda_z$  and frequency  $\omega_z \ll \omega_q$ . (b),(c) Phase-driving-induced slowdown of Rabi oscillations in qubit 1 (Q1). (b) We sweep  $\omega_z$  and measure the Pauli-spin-blockaded current  $I_{\text{norm}}$  normalized by the maximal current, proportional to the spin-flip probability, for different burst times  $t_b$ . The two regular Rabi peaks for  $Z = \lambda_z/\omega_z \lesssim 0.4$  curve up and thus slow down for increasing  $Z \gtrsim 0.4$ , following  $\omega_R = \lambda_x J_0(2Z)$ . At larger  $Z$ 's the peaks split up and higher harmonics result in nontrivial features that are captured by the simulation in (c) obtained from Eq. (1) with  $\lambda_x/2\pi = 29$  MHz,  $\lambda_z/2\pi = 30$  MHz, and  $\omega_q/2\pi = \omega_x/2\pi = 4.5$  GHz.

We demonstrate that the rich microscopic physics of hole nanostructures leads to a nontrivial response of the qubit state to these oscillating fields even at frequencies far detuned from the qubit energy. This anomalous response arises from a strong interplay between the phase and Rabi electrical drives in the *linear* regime. More specifically, by driving the qubit phase at radio-frequencies  $\omega_z$  in the MHz range, i.e., three orders of magnitude lower than the microwave GHz-range Larmor frequency of the qubit  $\omega_q$ , we controllably slow down the resonant Rabi oscillations, suppress them altogether at  $\omega_x = \omega_q$ , and revive them at sideband frequencies  $\omega_x = \omega_q \pm m\omega_z$ ,  $m \in \mathbb{N}^+$ . We observe this behavior reproducibly on two different devices. The suppression of Rabi frequency can be exploited to detect longitudinal interactions between spins and microwave resonators [14]. In future qubit processors using a global high-frequency driving field, sideband oscillations can provide ways to selectively address individual qubits by radio-frequency MHz signals, relieving demanding technological challenges for designing large-scale high-frequency circuits [50–54]. We also predict that our two-tone drive protects Rabi oscillations from noise as the periodic phase-driving gaps the Floquet spectrum of the system, similarly to Bloch bands in periodic lattices. This noise suppression is a valuable tool for dressed spin qubits [55–58] and for Floquet engineering high-fidelity quantum gates [59–64].

*Electrical manipulation of hole spins.*—A hole spin qubit in an external magnetic field  $\mathbf{B}$  is described by the Zeeman Hamiltonian  $H_q = \mathbf{b} \cdot \boldsymbol{\sigma}/2$ , where  $\mathbf{b} = \mu_B \mathbf{B} \cdot \hat{g}$  is the Zeeman vector,  $\hat{g}$  is the electrically tunable  $g$  tensor of the system, and  $\boldsymbol{\sigma}$  is the vector of Pauli matrices. Quite generally, an electrical pulse with frequency  $\omega$  applied to the system gives rise to an oscillating vector field  $\lambda \cos(\omega t)$  that directly couples to the qubit via  $H_d = \hbar \lambda \cdot \boldsymbol{\sigma} \cos(\omega t)$  due to the SOI. The vector  $\lambda \cos(\omega t)$  models the drive as a time-dependent Zeeman field acting on the qubit. Its direction

depends on the microscopic details of the nanostructure, and includes processes such as  $g$  tensor modulation and electric dipole spin resonance [39,41,42], while its amplitude scales linearly with the applied microwave field. These processes enable electrical manipulation of qubits with multiple driving frequencies and amplitudes. Transitions between spin up and down states occur for  $\lambda \perp \mathbf{b}$  (Rabi driving), while only the phase of the qubit is addressed [14,65–69] for  $\lambda \parallel \mathbf{b}$  (phase-driving). Interestingly, while phase-driving alone cannot induce Rabi oscillations, a radio-frequency phase pulse can significantly alter the dynamics of the qubit when acting together with a Rabi driving field.

We stress that all of our findings are linear in the driving field. Variations from linear regime were detected at large driving powers [6,70,71]. Nonlinearities  $\propto \lambda^2 \cos(\omega t)^2$  induced by excited states could also lead to a higher-harmonic response [48,49].

*Phase-driven qubits.*—We consider a qubit with GHz-range frequency  $\omega_q = |\mathbf{b}|/\hbar$ . A Rabi drive  $\lambda_x \cos(\omega_x t)$  with amplitude  $\lambda_x$  and frequency  $\omega_x = \omega_q - \Delta$  induces Rabi oscillations when the MHz-range detuning  $\Delta$  is small. This system exhibits Rabi oscillations with frequency  $\omega_R = \sqrt{\Delta^2 + \lambda_x^2}$  and maximal spin-flip probability  $P_R^{\max} = \lambda_x^2 / (\Delta^2 + \lambda_x^2)$ . We add an additional phase drive  $\lambda_z \cos(\omega_z t)$ , with amplitude  $\lambda_z$  and frequency  $\omega_z \sim \text{MHz}$ , far detuned from  $\omega_q$ . The two-tone Hamiltonian reads

$$\tilde{H} = \frac{\hbar\omega_q}{2}\sigma_z + \hbar\lambda_x\sigma_x \cos(\omega_x t) + \hbar\lambda_z\sigma_z \cos(\omega_z t). \quad (1)$$

The direction  $\hat{z}$  ( $\hat{x}$ ) is parallel (perpendicular) to  $\mathbf{b}$ , Fig. 1(a).

By moving to the rotating frame defined by the transformation  $U_r(t) = e^{-i\sigma_z[\omega_x t + 2Z \sin(\omega_z t)]/2}$  [14], which exactly accounts for phase-driving, and neglecting terms rotating at frequencies  $\sim 2\omega_x$ , we obtain

$$\tilde{H} = \frac{\hbar\Delta}{2}\sigma_z + \frac{\hbar\lambda_x}{2}J_0(2Z)\sigma_x + \hbar\lambda_x \sum_{n=1}^{\infty} \left( J_{2n}(2Z) \cos[2n\omega_z t]\sigma_x - J_{2n-1}(2Z) \sin[(2n-1)\omega_z t]\sigma_y \right), \quad (2)$$

with dimensionless parameter  $Z = \lambda_z/\omega_z$  and Bessel functions  $J_n$ . Without phase drive,  $\lambda_z = 0 \Rightarrow Z = 0$ , and since  $J_0(0) = 1$  and  $J_{n \neq 0}(0) = 0$ , Eq. (2) reduces to  $\tilde{H} = \hbar(\Delta\sigma_z + \lambda_x\sigma_x)/2$ , i.e., the rotating-frame Hamiltonian for Rabi-driven qubits in the rotating wave approximation (RWA), see the Supplemental Material (SM) [72].

Close to resonance  $\Delta \lesssim \omega_z, \lambda_x$  and at  $Z \ll 1$ , the term  $\propto J_0(2Z) = 1 - Z^2 + \mathcal{O}(Z^4)$  in  $\tilde{H}$  dominates the qubit dynamics, so that phase-driving has no effect when  $\omega_z \sim \omega_q \gg \lambda_z$ . Moreover, Rabi pulses with  $\omega_x \ll \omega_q$  are off-resonant and do not affect the qubit. These considerations justify using the Hamiltonian  $H$  in Eq. (1) also in general cases where  $\lambda_x$  ( $\lambda_z$ ) has additional components parallel (perpendicular) to  $\mathbf{b}$ . Finally, a relative phase

difference  $\varphi$  between the two driving signals is relevant at comparable values of  $\omega_x$  and  $\omega_z$  [14] but are negligible when  $\omega_z \ll \omega_x$ . Finite  $\varphi$ 's become relevant in the presence of noise, as discussed later.

*Sideband Rabi oscillations.*—We study the influence of the phase drive on the oscillations for resonant ( $\Delta = \omega_q - \omega_x = 0$ ) and nonresonant ( $\Delta \neq 0$ ) Rabi drives. In the resonant case and when  $\omega_z \gtrsim \lambda_x$ , one can simplify  $\tilde{H}$  in Eq. (2) by the RWA. The dominant contribution to  $\tilde{H}$  is the static  $n = 0$  component, yielding fully developed oscillations with frequency  $\omega_R = \lambda_x J_0(2Z)$ , see Figs. 1(b) and 1(c).

We verify this prediction experimentally in a hole spin qubit in two different Si FinFETs described in [12,27,73].

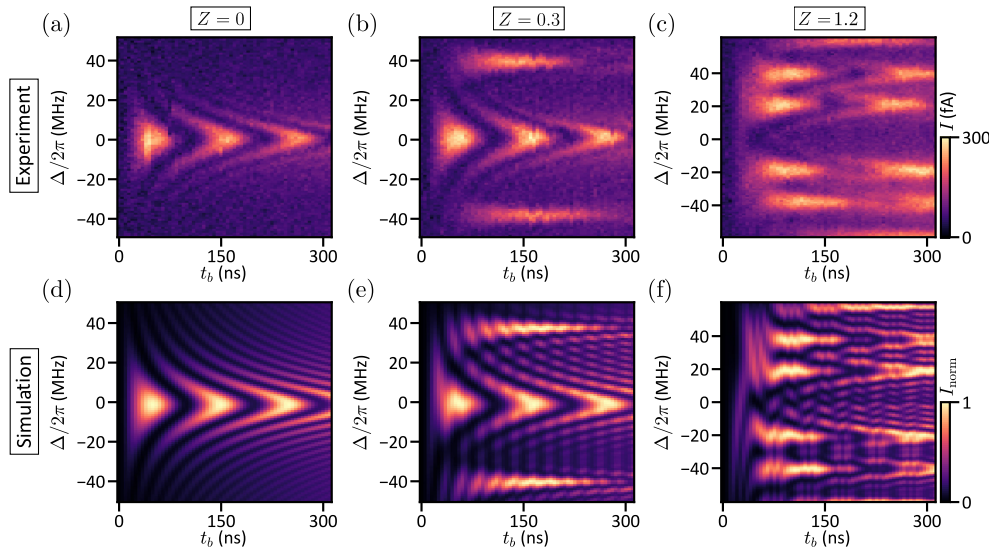


FIG. 2. Sideband Rabi oscillations in qubit 2 (Q2). (a)–(c) Spin precession for simultaneous microwave Rabi driving and radio-frequency phase-driving against burst time  $t_b$  and detuning  $\Delta$ . We show results for  $Z = 0$ ,  $Z = 0.3$ , and  $Z = 1.2$ . The typical chevron pattern centred at  $\Delta = 0$  in (a) is modified in (b),(c) by additional sidebands at  $\Delta/2\pi = \pm n \cdot \omega_z/2\pi = \pm n \cdot 40$  MHz and  $\pm n \cdot 20$  MHz, respectively. The  $\Delta = 0$  oscillations are slower in (b) and completely vanish in (c). (d)–(f) Simulations of the time evolution governed by Eq. (1), showing excellent agreement with experiments. We use  $\omega_q/2\pi = 4.95$  GHz,  $\lambda_x/2\pi = 10$  MHz for the three  $Z$  values and  $\lambda_z = 0$ ,  $\lambda_z/2\pi = 0.3\omega_z/2\pi = 12$  MHz,  $\lambda_z/2\pi = 1.2\omega_z/2\pi = 24$  MHz for (d)–(f), respectively.

Our first (second) qubit Q1 (Q2) is operated at  $\omega_q/2\pi = 4.5$  GHz ( $\omega_q/2\pi = 4.95$  GHz) corresponding to a  $g$  factor  $g = 2.14$  for  $B = 0.15$  T ( $g = 2.72$  for  $B = 0.13$  T);  $g$  depends on the gate potential  $V$  with sensitivity  $\partial g/\partial V \approx -0.05$  V $^{-1}$  ( $\partial g/\partial V \approx 0.41$  V $^{-1}$ ). Our qubits are initialized and read out via Pauli spin blockade and direct current integration, see [12,27]. Our system enables high-bandwidth phase-driving via the electrically tunable  $g$  tensor and Rabi driving via electric-dipole spin resonance. These contributions are generated by applying two oscillating electrical signals at different frequencies, Fig. 1(a). Generally these tones induce both Rabi and phase-driving; however, as discussed before, we discard the negligible contributions of far-detuned Rabi driving and nearly resonant phase-driving.

For the measurements in Fig. 1(b), we apply simultaneously a resonant Rabi drive with  $\omega_x = \omega_q$  and a phase drive with variable, far-detuned frequency  $\omega_z$  to Q1. We measure the qubit state after the burst time  $t_b$ . Rabi oscillations are observed along the vertical axis of Fig. 1(b). By sweeping  $\omega_z$ , we map out the dependence of  $\omega_R$  on  $Z = \lambda_z/\omega_z$ . We extract  $\lambda_x/2\pi \approx 30$  MHz from the period of the oscillations at large  $\omega_z$  and  $\lambda_z \approx \lambda_x$  from the decrease in Rabi frequency [ $\omega_R = \lambda_x J_0(2Z)$ ] as  $\omega_z$  decreases. We find good agreement between our measurement and the quantum dynamics simulated by using  $H$  in Eq. (1). We consistently reproduce this behavior in Q2 [72].

Remarkably, Eq. (2) predicts the vanishing of the fundamental Rabi oscillations, i.e.,  $\omega_R = \lambda_x J_0(2Z_j) = 0$ , with  $2Z_j$  denoting the  $j$ th root of  $J_0$ . The first root is  $Z_1 \approx 1.2 \rightarrow \lambda_z \approx 1.2\omega_z$  and is clearly observed in our

experiments. At  $Z = 1.2$ , higher harmonics ( $n \geq 1$ ) in  $\tilde{H}$  dominate the dynamics and determine the nontrivial time evolution shown in Fig. 1.

Higher harmonics are crucial to understand the Rabi sidebands appearing in the nonresonant case ( $\Delta \neq 0$ ), shown in Figs. 2(b) and 2(c). At small values of  $\Delta \ll \lambda_x$ , the Rabi frequency increases as  $\omega_R = \sqrt{\Delta^2 + \lambda_x^2 J_0(2Z)^2}$ , resulting in the typical chevron pattern, and suppressing the oscillations at large  $\Delta$ 's. However, when  $\lambda_z \approx \omega_z$ , oscillations are revived at finite  $\Delta$ 's. In particular, at  $\Delta = \pm m\omega_z$ , the system is resonant with the  $m$ th harmonic in Eq. (2), and sideband oscillations with frequencies  $\omega_R^m = \lambda_x J_m(2Z)$  are restored.

In Fig. 2, we show measurements and simulations of Rabi oscillations against  $\Delta$  at different values of  $Z$  for Q2. The Rabi chevron in (a) is modified by phase-driving. In (b), we consider  $Z = 0.3$ , and we observe the appearance of sideband resonances at frequencies  $\pm \omega_z/2\pi = \pm 40$  MHz. In (c), by reducing  $\omega_z$  to  $\omega_z/2\pi = 20$  MHz and increasing  $\lambda_z$ , we reach  $Z = 1.2$ , where the resonant oscillations at  $\Delta = 0$  vanish and only sideband oscillations remain. As shown in Figs. 2(d)–2(f), these sidebands are well explained by our model, which is linear in the driving field amplitudes. We emphasize that in contrast to nonlinear driving, where the  $\Delta = 0$  resonance does not disappear and sidebands oscillations appear at fixed frequencies  $\omega_x = \omega_q/m$  with  $m \in \mathbb{N}^+$ , by operating our qubit at  $Z = 1.2$  we remove the  $\Delta = 0$  oscillations and still fully control the sideband frequencies  $\Delta = \pm m\omega_z = \pm m\lambda_z/1.2$  by varying the amplitude  $\lambda_z$  of the radio-frequency pulse. Operating at

larger  $\lambda_z$  substantially improves the fidelity of the sidebands oscillations; see the SM [72].

Our two-tone driving scheme dynamically shifts the qubit frequency to higher harmonics without critically altering the static properties of the qubit. This can reduce frequency-crowding issues in dense large-scale quantum processors and enable individual qubit addressability in global microwave fields by MHz circuits.

*Effects of noise.*—The coupling to the environment causes decoherence and damps Rabi oscillations in a time  $T_2^R$ . Because of the limited time window of the transport readout, we cannot measure  $T_2^R$  in our current devices. However, we estimate that  $T_2^R$  is dominated by random fields coupled to  $\lambda_x$ , yielding  $T_2^R \sim 25 \mu\text{s}$  [72]. These slow-dynamics fields originate from different microscopic sources [24,25,34,62,74–76]. We model them by the noise Hamiltonian  $H_N = \cos(\omega_x t) \mathbf{h} \cdot \boldsymbol{\sigma}$ , with a quasistatic, Gaussian-distributed stochastic vector  $\mathbf{h}$  modulated by the Rabi drive having zero mean and covariance matrix  $\Sigma_{ij} = \delta_{ij} \bar{\sigma}^2$ . Variants of this model originating from the  $1/\omega$  tail, typical of charge noise, are discussed in [72].

After ensemble averaging and at resonance  $\Delta = 0$ , we find that for conventional Rabi driving  $H_N$  suppresses the Rabi oscillations as [72]

$$P_R(t) = \frac{1}{2} \left[ 1 - e^{-(t/T_2^R)^2} \cos(\omega_R t) \right], \quad (3)$$

with  $T_2^R = \sqrt{2\hbar/\bar{\sigma}}$ . To better illustrate this decay in Fig. 3(a) (black curve) we consider a  $T_2^R$  shorter than in our device but typical e.g., of Ge/Si nanowires [6]. The decay time  $T_2^R$  is larger than the dephasing time  $T_2^*$  and determines the lifetime of dressed spin qubits [55–58] utilizing nearly resonant always-on global microwave fields. However, when the SOI is large  $T_2^R$  is significantly shortened and can become comparable to  $T_2^*$  [5–7].

*Protection of Rabi oscillations from noise.*—We simulate the effect of an additional phase pulse with  $\lambda_z \ll \lambda_x$  at frequency  $\omega_z \approx \lambda_x$ . In this regime, the higher harmonics in Eq. (2) have a significant effect even at  $\Delta = 0$ . As shown in Fig. 3(a), even a small phase-driving (red curve) decouples Rabi oscillations from noise and substantially enhances  $T_2^R$ .

The persistent oscillations can be understood in terms of Floquet modes  $|0_F\rangle, |1_F\rangle$  [72,77–79]. These are eigenstates of the Floquet operator  $U(T) = U_r(T) T e^{-i \int_0^T \tilde{H}(\tau) d\tau / \hbar}$  with eigenvalues  $e^{-i\omega_F^0 T}, e^{-i\omega_F^1 T}$ , respectively. Here,  $T e$  is the time-ordered exponential  $T = 2\pi/\omega_z$ , and  $U_r$  transforms the system back to the lab frame.

The eigenvalues and eigenvectors of  $U(T)$  are shown in Fig. 3(b). First, in contrast to the usual Rabi driving, when a phase-driving pulse is applied at frequencies comparable to  $\lambda_x$  and is in-phase with the Rabi drive, the spin states in the lab frame coincide with the Floquet modes, i.e.,  $|\uparrow\rangle = |0_F\rangle$ ,  $|\downarrow\rangle = |1_F\rangle$  (magenta line). Second, phase-driving opens a

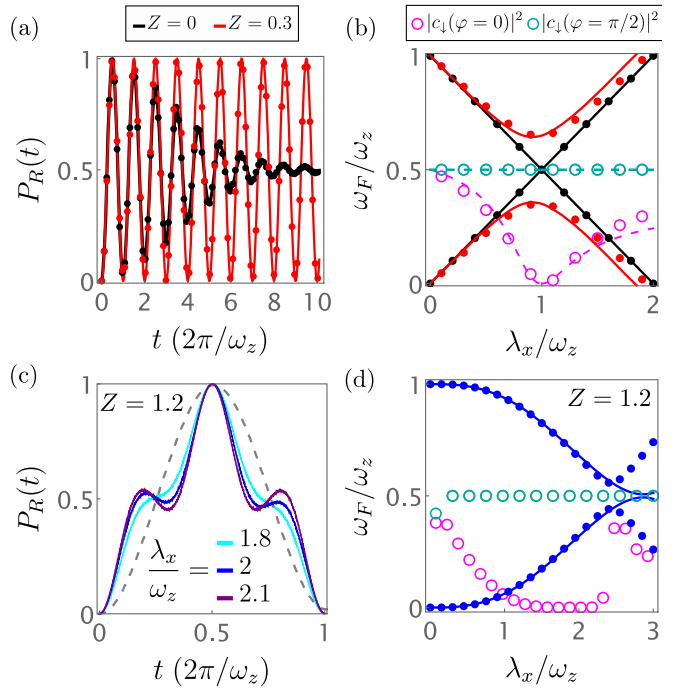


FIG. 3. (a) Simulated phase-driving-induced undamped Rabi oscillations at  $\omega_z = \lambda_x$ . Black (red) dots denote Rabi probability averaged over  $N = 10^3$  realizations of the noise Hamiltonian  $H_N$  for  $\lambda_z = 0$  ( $\lambda_z = 0.3\omega_z$ ) picked from a Gaussian distribution with zero mean and standard deviation  $\bar{\sigma} = 0.05\hbar\omega_z$ . (c) Noisy Rabi oscillation at  $Z = 1.2$  and various  $\lambda_x/\omega_z$  ratios. For reference, we show the gray dashed line, corresponding to the red line in (a). (b),(d) Floquet spectra against  $\lambda_x/\omega_z$ . (b) Solid black (red) dots show numerically computed Floquet energies  $\omega_F$  at  $\lambda_z = 0$  ( $\lambda_z = 0.3\omega_z$ ); the lines denote the approximation in Eq. (4). Magenta (cyan) circles exhibit the probability  $|c_{\downarrow}|^2 = |\langle \downarrow | 0_F \rangle|^2$  for a two-tone relative phase  $\varphi = 0$  ( $\varphi = \pi/2$ ). Dashed lines show Eq. (5). (d) Blue dots show the Floquet spectrum at  $Z = 1.2$ , while the lines display the fitting formula  $\omega_F^{0,1} = \pm\omega_z [0.084(\lambda_x/\omega_z)^3 - 0.022(\lambda_x/\omega_z)^4] \bmod (\omega_z)$ . We use  $\omega_q = 10^3\omega_z$ .

gap of size  $\omega_F^1 - \omega_F^0 \approx \lambda_z$  in the Floquet spectrum (black and red lines) that protects the system from moderate noise sources with  $\bar{\sigma} \lesssim \lambda_z$ . For  $\lambda_z \ll \lambda_x \sim \omega_z$ , the Floquet eigenenergies are [72]

$$\omega_F^{0,1} = \pm \frac{1}{2} \left[ \omega_z + \sqrt{(\lambda_x - \omega_z)^2 + \frac{\lambda_x^2 \lambda_z^2}{\omega_z^2}} \right] \bmod (\omega_z). \quad (4)$$

The long-lived Rabi oscillations depend on the gapped Floquet spectrum and the possibility of preparing Floquet eigenmodes. In our devices,  $T_2^R$  is determined by the dephasing of Floquet modes. Thus by initializing the system in a Floquet eigenstate, we filter out the dominant noise source. In this case,  $T_2^R$  depends only on relaxation of Floquet eigenmodes. However, in analogy to disorder potentials in

Bloch bands, transitions to other eigenstates are suppressed provided that the standard deviation of the disorder be smaller than the energy band gap. This parallel allows us to interpret the oscillations shown by red curves in Fig. 3(a) as the temporal evolution of individual Floquet modes. We estimate that relaxation yields a slow power-law decay of the oscillations, with time constant  $\sim 10T_2^R$ , see the SM [72].

In Fig. 3(b), we show that a relative, experimentally tunable phase  $\varphi$  between the Rabi and phase tones can select arbitrary superpositions of Floquet states (magenta and cyan curves). The amplitudes  $c_s = \langle s | 0_F \rangle$  between spin  $|s = \uparrow\downarrow\rangle$  and Floquet states  $|0_F\rangle$  are [72]

$$c_{\uparrow\downarrow}(\varphi) \approx \frac{\cos(\theta) \pm \sin(\theta) e^{i\varphi}}{\sqrt{2}}, \quad \tan(2\theta) = \frac{\lambda_x \lambda_z}{\omega_z |\lambda_x - \omega_z|}. \quad (5)$$

For strong phase-drivings, where  $\lambda_z \sim \lambda_x$ , Eqs. (4) and (5) are inaccurate, but simulations still predict long-lived oscillations and gapped Floquet spectrum. For example, in Figs. 3(c) and 3(d) we examine the oscillations and the Floquet spectrum at  $Z = 1.2$ . The Floquet bands touch at  $\lambda_x = 0 \bmod (\omega_z)$ ; at  $\lambda_x \gtrsim \omega_z$ , the gap becomes significant and long-lived oscillations persist for a wide range of parameters. Because of the strong phase-driving the oscillations are not sinusoidal. Their peculiar shape probes the temporal structure of Floquet modes and is shown in Fig. 3(d) for different  $\lambda_x$ 's.

We envision that the phase-driving-induced stabilization of Floquet modes will open a wide range of opportunities to optimize dressed qubits and prepare exotic states in Floquet metamaterials.

*Conclusion.*—We demonstrated that radio-frequency phase-driving of hole spin qubits induces collapse and revival of Rabi oscillations, yielding oscillations at sidebands of the qubit frequency. We show theoretically that phase-driving also leads to long-lived Rabi oscillations in noisy qubits. Phase-driving provides an alternative way of implementing individual addressability in global microwave fields in future large-scale qubit architectures and Floquet engineering high-fidelity gates.

The data in the figures of this paper are available at the Zenodo repository at [80].

We thank T. Berger for the rendering of our FinFET device. We acknowledge support by the cleanroom operation team, particularly U. Drechsler, A. Olziersky, and D. D. Pineda, at the IBM Binnig and Rohrer Nanotechnology Center, and technical support at the University of Basel by S. Martin and M. Steinacher. L. C. C. acknowledges support by a Swiss NSF mobility fellowship (P2BSP2200127). This work was supported by the Swiss National Science Foundation (NCCR SPIN) Grant No. 51NF40-180604, by the EU H2020 European Microkelvin Platform (EMP) Grant No. 824109, and by the Conselho Nacional de Pesquisas (CNPq) Grant No. 301595/2022-4.

\* stefano.bosco@unibas.ch

<sup>†</sup>Present address: RIKEN, Center for Emergent Matter Science (CEMS), Wako-shi, Saitama 351-0198, Japan.

- [1] C. Kloeffel and D. Loss, Prospects for spin-based quantum computing in quantum dots, *Annu. Rev. Condens. Matter Phys.* **4**, 51 (2013).
- [2] G. Scappucci, C. Kloeffel, F. A. Zwanenburg, D. Loss, M. Myronov, J.-J. Zhang, S. De Franceschi, G. Katsaros, and M. Veldhorst, The germanium quantum information route, *Nat. Rev. Mater.* **6**, 926 (2021).
- [3] Y. Fang, P. Philippopoulos, D. Culcer, W. A. Coish, and S. Chesi, Recent advances in hole-spin qubits, *Mater. Quantum Technol.* **3**, 012003 (2023).
- [4] N. W. Hendrickx, W. I. L. Lawrie, M. Russ, F. van Riggelen, S. L. de Snoo, R. N. Schouten, A. Sammak, G. Scappucci, and M. Veldhorst, A four-qubit germanium quantum processor, *Nature (London)* **591**, 580 (2021).
- [5] K. Wang, G. Xu, F. Gao, H. Liu, R.-L. Ma, X. Zhang, Z. Wang, G. Cao, T. Wang, J.-J. Zhang, D. Culcer, X. Hu, H.-W. Jiang, H.-O. Li, G.-C. Guo, and G.-P. Guo, Ultrafast coherent control of a hole spin qubit in a germanium quantum dot, *Nat. Commun.* **13**, 206 (2022).
- [6] F. N. M. Froning, L. C. Camenzind, O. A. H. van der Molen, A. Li, E. P. A. M. Bakkers, D. M. Zumbühl, and F. R. Braakman, Ultrafast hole spin qubit with gate-tunable spin-orbit switch functionality, *Nat. Nanotechnol.* **16**, 308 (2021).
- [7] H. Liu, K. Wang, F. Gao, J. Leng, Y. Liu, Y.-C. Zhou, G. Cao, T. Wang, J. Zhang, P. Huang, H.-O. Li, and G.-P. Guo, Ultrafast and electrically tunable rabi frequency in a germanium hut wire hole spin qubit, *Nano Lett.* **23**, 3810 (2023).
- [8] H. Watzinger, J. Kukucka, L. Vukušić, F. Gao, T. Wang, F. Schäffler, J.-J. Zhang, and G. Katsaros, A germanium hole spin qubit, *Nat. Commun.* **9**, 3902 (2018).
- [9] N. W. Hendrickx, W. I. L. Lawrie, L. Petit, A. Sammak, G. Scappucci, and M. Veldhorst, A single-hole spin qubit, *Nat. Commun.* **11**, 3478 (2020).
- [10] N. Hendrickx, D. Franke, A. Sammak, G. Scappucci, and M. Veldhorst, Fast two-qubit logic with holes in germanium, *Nature (London)* **577**, 487 (2020).
- [11] R. Maurand, X. Jehl, D. Kotekar-Patil, A. Corra, H. Bohuslavskyi, R. Laviéville, L. Hutin, S. Barraud, M. Vinet, M. Sanquer, and S. De Franceschi, A CMOS silicon spin qubit, *Nat. Commun.* **7**, 1 (2016).
- [12] L. C. Camenzind, S. Geyer, A. Fuhrer, R. J. Warburton, D. M. Zumbühl, and A. V. Kuhlmann, A hole spin qubit in a fin field-effect transistor above 4 kelvin, *National electronics review* **5**, 178 (2022).
- [13] C. X. Yu, S. Zihlmann, J. C. Abadillo-Urbel, V. P. Michal, N. Rambal, H. Niebojewski, T. Bedecarrats, M. Vinet, É. Dumur, M. Filippone, B. Bertrand, S. De Franceschi, Y.-M. Niquet, and R. Maurand, Strong coupling between a photon and a hole spin in silicon, *Nat. Nanotechnol.* **18**, 741 (2023).
- [14] S. Bosco, P. Scarlino, J. Klinovaja, and D. Loss, Fully tunable longitudinal spin-photon interactions in Si and Ge quantum dots, *Phys. Rev. Lett.* **129**, 066801 (2022).
- [15] V. P. Michal, J. C. Abadillo-Urbel, S. Zihlmann, R. Maurand, Y.-M. Niquet, and M. Filippone, Tunable hole spin-photon

- interaction based on g-matrix modulation, *Phys. Rev. B* **107**, L041303 (2023).
- [16] S. G. J. Philips, M. T. Madzik, S. V. Amitonov, S. L. de Snoo, M. Russ, N. Kalhor, C. Volk, W. I. L. Lawrie, D. Brousse, L. Tryputen, B. P. Wuett, A. Sammak, M. Veldhorst, G. Scappucci, and L. M. K. Vandersypen, Universal control of a six-qubit quantum processor in silicon, *Nature (London)* **609**, 919 (2022).
- [17] A. R. Mills, C. R. Guinn, M. J. Gullans, A. J. Sigillito, M. M. Feldman, E. Nielsen, and J. R. Petta, Two-qubit silicon quantum processor with operation fidelity exceeding 99%, *Sci. Adv.* **8**, eabn5130 (2022).
- [18] A. Noiri, K. Takeda, T. Nakajima, T. Kobayashi, A. Sammak, G. Scappucci, and S. Tarucha, Fast universal quantum gate above the fault-tolerance threshold in silicon, *Nature (London)* **601**, 338 (2022).
- [19] F. N. M. Froning, M. J. Rančić, B. Hetényi, S. Bosco, M. K. Rehmann, A. Li, E. P. A. M. Bakkers, F. A. Zwanenburg, D. Loss, D. M. Zumbühl, and F. R. Braakman, Strong spin-orbit interaction and g-factor renormalization of hole spins in Ge/Si nanowire quantum dots, *Phys. Rev. Res.* **3**, 013081 (2021).
- [20] S. D. Liles, F. Martins, D. S. Miserev, A. A. Kiselev, I. D. Thorvaldson, M. J. Rendell, I. K. Jin, F. E. Hudson, M. Veldhorst, K. M. Itoh, O. P. Sushkov, T. D. Ladd, A. S. Dzurak, and A. R. Hamilton, Electrical control of the g tensor of the first hole in a silicon MOS quantum dot, *Phys. Rev. B* **104**, 235303 (2021).
- [21] K. Hudson, A. Srinivasan, D. Miserev, Q. Wang, O. Klochan, O. Sushkov, I. Farrer, D. Ritchie, and A. Hamilton, Observation of oscillating g-factor anisotropy arising from strong crystal lattice anisotropy in GaAs spin-3/2 hole quantum point contacts, *arXiv:2211.00253*.
- [22] C. Adelsberger, S. Bosco, J. Klinovaja, and D. Loss, Enhanced orbital magnetic field effects in Ge hole nanowires, *Phys. Rev. B* **106**, 235408 (2022).
- [23] S. Bosco, M. Benito, C. Adelsberger, and D. Loss, Squeezed hole spin qubits in Ge quantum dots with ultrafast gates at low power, *Phys. Rev. B* **104**, 115425 (2021).
- [24] S. Bosco and D. Loss, Fully tunable hyperfine interactions of hole spin qubits in Si and Ge quantum dots, *Phys. Rev. Lett.* **127**, 190501 (2021).
- [25] J. Fischer, W. A. Coish, D. V. Bulaev, and D. Loss, Spin decoherence of a heavy hole coupled to nuclear spins in a quantum dot, *Phys. Rev. B* **78**, 155329 (2008).
- [26] J. H. Prechtel, A. V. Kuhlmann, J. Houel, A. Ludwig, S. R. Valentin, A. D. Wieck, and R. J. Warburton, Decoupling a hole spin qubit from the nuclear spins, *Nat. Mater.* **15**, 981 (2016).
- [27] S. Geyer, B. Hetényi, S. Bosco, L. C. Camenzind, R. S. Egeli, A. Fuhrer, D. Loss, R. J. Warburton, D. M. Zumbühl, and A. V. Kuhlmann, Two-qubit logic with anisotropic exchange in a fin field-effect transistor, *arXiv:2212.02308*.
- [28] G. Katsaros, J. Kukučka, L. Vukušić, H. Watzinger, F. Gao, T. Wang, J.-J. Zhang, and K. Held, Zero field splitting of heavy-hole states in quantum dots, *Nano Lett.* **20**, 5201 (2020).
- [29] B. Hetényi, S. Bosco, and D. Loss, Anomalous zero-field splitting for hole spin qubits in Si and Ge quantum dots, *Phys. Rev. Lett.* **129**, 116805 (2022).
- [30] S. Bosco, B. Hetényi, and D. Loss, Hole spin qubits in Si finfets with fully tunable spin-orbit coupling and sweet spots for charge noise, *PRX Quantum* **2**, 010348 (2021).
- [31] S. Bosco and D. Loss, Hole spin qubits in thin curved quantum wells, *Phys. Rev. Appl.* **18**, 044038 (2022).
- [32] C. Adelsberger, M. Benito, S. Bosco, J. Klinovaja, and D. Loss, Hole-spin qubits in Ge nanowire quantum dots: Interplay of orbital magnetic field, strain, and growth direction, *Phys. Rev. B* **105**, 075308 (2022).
- [33] N. Piot, B. Brun, V. Schmitt, S. Zihlmann, V. P. Michal, A. Apra, J. C. Abadillo-Uriel, X. Jehl, B. Bertrand, H. Niebojewski, L. Hutin, M. Vinet, M. Urdampilleta, T. Meunier, Y.-M. Niquet, R. Maurand, and S. D. Franceschi, A single hole spin with enhanced coherence in natural silicon, *Nat. Nanotechnol.* **17**, 1072 (2022).
- [34] Z. Wang, E. Marcellina, A. R. Hamilton, J. H. Cullen, S. Rogge, J. Salfi, and D. Culcer, Optimal operation points for ultrafast, highly coherent Ge hole spin-orbit qubits, *npj Quantum Inf.* **7**, 54 (2021).
- [35] C.-A. Wang, G. Scappucci, M. Veldhorst, and M. Russ, Modelling of planar germanium hole qubits in electric and magnetic fields, *arXiv:2208.04795*.
- [36] N. Ares, G. Katsaros, V. N. Golovach, J. J. Zhang, A. Prager, L. I. Glazman, O. G. Schmidt, and S. De Franceschi, Sige quantum dots for fast hole spin Rabi oscillations, *Appl. Phys. Lett.* **103**, 263113 (2013).
- [37] A. Crippa, R. Maurand, L. Bourdet, D. Kotekar-Patil, A. Amisse, X. Jehl, M. Sanquer, R. Laviéville, H. Bohuslavskyi, L. Hutin, S. Barraud, M. Vinet, Y.-M. Niquet, and S. De Franceschi, Electrical spin driving by g-matrix modulation in spin-orbit qubits, *Phys. Rev. Lett.* **120**, 137702 (2018).
- [38] B. Venitucci, L. Bourdet, D. Pouzada, and Y.-M. Niquet, Electrical manipulation of semiconductor spin qubits within the g-matrix formalism, *Phys. Rev. B* **98**, 155319 (2018).
- [39] V. N. Golovach, M. Borhani, and D. Loss, Electric-dipole-induced spin resonance in quantum dots, *Phys. Rev. B* **74**, 165319 (2006).
- [40] K. C. Nowack, F. H. L. Koppens, Y. V. Nazarov, and L. M. K. Vandersypen, Coherent control of a single electron spin with electric fields, *Science* **318**, 1430 (2007).
- [41] C. Kloeffel, M. Trif, and D. Loss, Strong spin-orbit interaction and helical hole states in ge/si nanowires, *Phys. Rev. B* **84**, 195314 (2011).
- [42] C. Kloeffel, M. J. Rancic, and D. Loss, Direct Rashba spin-orbit interaction in Si and Ge nanowires with different growth directions, *Phys. Rev. B* **97**, 235422 (2018).
- [43] A. Blais, A. L. Grimsom, S. M. Girvin, and A. Wallraff, Circuit quantum electrodynamics, *Rev. Mod. Phys.* **93**, 025005 (2021).
- [44] D. Leibfried, R. Blatt, C. Monroe, and D. Wineland, Quantum dynamics of single trapped ions, *Rev. Mod. Phys.* **75**, 281 (2003).
- [45] W. Gilbert *et al.*, On-demand electrical control of spin qubits, *Nat. Nanotechnol.* **18**, 131 (2023).
- [46] J. J. Pla, K. Y. Tan, J. P. Dehollain, W. H. Lim, J. J. L. Morton, D. N. Jamieson, A. S. Dzurak, and A. Morello, A single-atom electron spin qubit in silicon, *Nature (London)* **489**, 541 (2012).

- [47] F. H. L. Koppens, C. Buizert, K. J. Tielrooij, I. T. Vink, K. C. Nowack, T. Meunier, L. P. Kouwenhoven, and L. M. K. Vandersypen, Driven coherent oscillations of a single electron spin in a quantum dot, *Nature (London)* **442**, 766 (2006).
- [48] P. Scarlino, E. Kawakami, D. R. Ward, D. E. Savage, M. G. Lagally, M. Friesen, S. N. Coppersmith, M. A. Eriksson, and L. M. K. Vandersypen, Second-harmonic coherent driving of a spin qubit in a Si/SiGe quantum dot, *Phys. Rev. Lett.* **115**, 106802 (2015).
- [49] S. Stufler, P. Machnikowski, P. Ester, M. Bichler, V. M. Axt, T. Kuhn, and A. Zrenner, Two-photon Rabi oscillations in a single  $\text{In}_x\text{Ga}_{1-x}\text{As}/\text{GaAs}$  quantum dot, *Phys. Rev. B* **73**, 125304 (2006).
- [50] W. I. L. Lawrie, M. Rimbach-Russ, F. v. Riggelen, N. W. Hendrickx, S. L. d. Snoo, A. Sammak, G. Scappucci, J. Helsen, and M. Veldhorst, Simultaneous single-qubit driving of semiconductor spin qubits at the fault-tolerant threshold, *Nat. Commun.* **14**, 3617 (2023).
- [51] M. Veldhorst, H. G. J. Eenink, C. H. Yang, and A. S. Dzurak, Silicon CMOS architecture for a spin-based quantum computer, *Nat. Commun.* **8**, 1766 (2017).
- [52] L. M. K. Vandersypen, H. Bluhm, J. S. Clarke, A. S. Dzurak, R. Ishihara, A. Morello, D. J. Reilly, L. R. Schreiber, and M. Veldhorst, Interfacing spin qubits in quantum dots and donors:—hot, dense, and coherent, *npj Quantum Inf.* **3**, 34 (2017).
- [53] Z. György, A. Pályi, and G. Széchenyi, Electrically driven spin resonance with bichromatic driving, *Phys. Rev. B* **106**, 155412 (2022).
- [54] F. Vigneau, F. Fedele, A. Chatterjee, D. Reilly, F. Kuemmeth, M. F. Gonzalez-Zalba, E. Laird, and N. Ares, Probing quantum devices with radio-frequency reflectometry, *Appl. Phys. Rev.* **10**, 021305 (2023).
- [55] A. Laucht, R. Kalra, S. Simmons, J. P. Dehollain, J. T. Muñonen, F. A. Mohiyaddin, S. Freer, F. E. Hudson, K. M. Itoh, D. N. Jamieson, J. C. McCallum, A. S. Dzurak, and A. Morello, A dressed spin qubit in silicon, *Nat. Nanotechnol.* **12**, 61 (2017).
- [56] A. E. Seedhouse, I. Hansen, A. Laucht, C. H. Yang, A. S. Dzurak, and A. Saraiva, Quantum computation protocol for dressed spins in a global field, *Phys. Rev. B* **104**, 235411 (2021).
- [57] I. Hansen, A. E. Seedhouse, A. Saraiva, A. Laucht, A. S. Dzurak, and C. H. Yang, Pulse engineering of a global field for robust and universal quantum computation, *Phys. Rev. A* **104**, 062415 (2021).
- [58] I. Hansen, A. E. Seedhouse, K. W. Chan, F. E. Hudson, K. M. Itoh, A. Laucht, A. Saraiva, C. H. Yang, and A. S. Dzurak, Implementation of an advanced dressing protocol for global qubit control in silicon, *Appl. Phys. Rev.* **9**, 031409 (2022).
- [59] X. Xue, M. Russ, N. Samkharadze, B. Undseth, A. Sammak, G. Scappucci, and L. M. K. Vandersypen, Quantum logic with spin qubits crossing the surface code threshold, *Nature (London)* **601**, 343 (2022).
- [60] E. Boyers, M. Pandey, D. K. Campbell, A. Polkovnikov, D. Sels, and A. O. Sushkov, Floquet-engineered quantum state manipulation in a noisy qubit, *Phys. Rev. A* **100**, 012341 (2019).
- [61] F. Petiziol, B. Dive, F. Mintert, and S. Wimberger, Fast adiabatic evolution by oscillating initial Hamiltonians, *Phys. Rev. A* **98**, 043436 (2018).
- [62] C. H. Yang, K. W. Chan, R. Harper, W. Huang, T. Evans, J. C. C. Hwang, B. Hensen, A. Laucht, T. Tanttu, F. E. Hudson, S. T. Flammia, K. M. Itoh, A. Morello, S. D. Bartlett, and A. S. Dzurak, Silicon qubit fidelities approaching incoherent noise limits via pulse engineering, *National electronics review* **2**, 151 (2019).
- [63] J. Zeng, C. H. Yang, A. S. Dzurak, and E. Barnes, Geometric formalism for constructing arbitrary single-qubit dynamically corrected gates, *Phys. Rev. A* **99**, 052321 (2019).
- [64] M. Rimbach-Russ, S. G. Philips, X. Xue, and L. M. Vandersypen, Simple framework for systematic high-fidelity gate operations, *arXiv:2211.16241*.
- [65] P.-M. Billangeon, J. S. Tsai, and Y. Nakamura, Circuit-QED-based scalable architectures for quantum information processing with superconducting qubits, *Phys. Rev. B* **91**, 094517 (2015).
- [66] S. Richer and D. DiVincenzo, Circuit design implementing longitudinal coupling: A scalable scheme for superconducting qubits, *Phys. Rev. B* **93**, 134501 (2016).
- [67] R. Ruskov and C. Tahan, Modulated longitudinal gates on encoded spin qubits via curvature couplings to a superconducting cavity, *Phys. Rev. B* **103**, 035301 (2021).
- [68] R. Ruskov and C. Tahan, Quantum-limited measurement of spin qubits via curvature couplings to a cavity, *Phys. Rev. B* **99**, 245306 (2019).
- [69] C. G. L. Böttcher, S. P. Harvey, S. Fallahi, G. C. Gardner, M. J. Manfra, U. Vool, S. D. Bartlett, and A. Yacoby, Parametric longitudinal coupling between a high-impedance superconducting resonator and a semiconductor quantum dot singlet-triplet spin qubit, *Nat. Commun.* **13**, 4773 (2022).
- [70] J. Yoneda, K. Takeda, T. Otsuka, T. Nakajima, M. R. Delbecq, G. Allison, T. Honda, T. Kodera, S. Oda, Y. Hoshi, N. Usami, K. M. Itoh, and S. Tarucha, A quantum-dot spin qubit with coherence limited by charge noise and fidelity higher than 99.9%, *Nat. Nanotechnol.* **13**, 102 (2018).
- [71] B. Undseth, X. Xue, M. Mehmandoost, M. Russ, N. Samkharadze, A. Sammak, V. V. Dobrovitski, G. Scappucci, and L. M. Vandersypen, Nonlinear response and crosstalk of strongly driven silicon spin qubits, *arXiv:2205.04905*.
- [72] See Supplemental Material at <http://link.aps.org/supplemental/10.1103/PhysRevLett.131.197001> for we show additional experimental data of phase driving obtained in our two devices.
- [73] S. Geyer, L. C. Camenzind, L. Czornomaz, V. Deshpande, A. Fuhrer, R. J. Warburton, D. M. Zumbühl, and A. V. Kuhlmann, Self-aligned gates for scalable silicon quantum computing, *Appl. Phys. Lett.* **118**, 104004 (2021).
- [74] S. Chesi, L.-P. Yang, and D. Loss, Dephasing due to nuclear spins in large-amplitude electric dipole spin resonance, *Phys. Rev. Lett.* **116**, 066806 (2016).
- [75] L. Cywiński, R. M. Lutchyn, C. P. Nave, and S. Das Sarma, How to enhance dephasing time in superconducting qubits, *Phys. Rev. B* **77**, 174509 (2008).
- [76] F. H. L. Koppens, D. Klauser, W. A. Coish, K. C. Nowack, L. P. Kouwenhoven, D. Loss, and L. M. K. Vandersypen,

- Universal phase shift and nonexponential decay of driven single-spin oscillations, *Phys. Rev. Lett.* **99**, 106803 (2007).
- [77] M. Bukov, L. D'Alessio, and A. Polkovnikov, Universal high-frequency behavior of periodically driven systems: From dynamical stabilization to floquet engineering, *Adv. Phys.* **64**, 139 (2015).
- [78] M. S. Rudner and N. H. Lindner, Band structure engineering and non-equilibrium dynamics in floquet topological insulators, *Nat. Rev. Phys.* **2**, 229 (2020).
- [79] D. Zeuch, F. Hassler, J. J. Slim, and D. P. DiVincenzo, Exact rotating wave approximation, *Ann. Phys. (Amsterdam)* **423**, 168327 (2020).
- [80] <https://zenodo.org/records/8033384>.